AIMS Mathematics, 8(1): 2419–2434.
DOI: 10.3934/math.2023125
Received: 22 August 2022
Revised: 14 October 2022
Accepted: 19 October 2022
Published: 02 November 2022

http://www.aimspress.com/journal/Math

Research article

An extension of mathematical model for severity of rice blast disease

Saharat Tabonglek, Amir Khan and Usa Wannasingha Humphries*

Department of Mathematics, Faculty of Science, King Mongkut's University of Technology Thonburi, Bangkok 10140, Thailand

* **Correspondence:** Email: usa.wan@kmutt.ac.th.

Abstract: This paper aims to extend the spore dispersal model to the Healthy-Latent-Infectious-Removed (HLIR) epidemic model for assessing the severity of rice blast disease. The model was solved by the Finite Difference Method (FDM). The results of the model were compared to data from the Prachinburi Rice Research Center (PRRC) on the severity of rice blast disease. Because of a small error, the comparison results showed good agreement between the PRRC data and the simulation by looking at the value of Willmott's index of agreement (d). The first bed d was 0.7166, while the second bed d was 0.6421, indicating the model's performance. Furthermore, the optimal parameter, the fraction of spores deposited on the crop, was determined to be 0.173 and 0.016 for beds 1 and 2, respectively. The model can simulate and analyze rice blast outbreaks for educational purposes in future preparedness planning.

Keywords: disease severity; epidemic model; plant disease; rice blast disease; spore dispersal
Mathematics Subject Classification: 92D25, 92D30

1. Introduction

Rice is a staple meal for many people around the world. Rice blast disease is one of the diseases that reduce rice yields [1]. Moreover, rice blast epidemics have caused crop yield losses ranging from 50–100% in various parts of the world, compared to 20–50% by sheath blight, 50–70% by brown spot disease, 25% by bacterial leaf blight, and 20–80% by sheath rot disease [2]. The disease severity is the percentage of the total area infected that can tell the behavior of an outbreak. Many factors affect the outbreak, including weather factors such as temperature, relative humidity, leaf wetness, or the spore dispersion which can disperse depending on many factors such as wind, water, insect, animals, and humans [3, 4].

Many researchers constructed and developed a mathematical model to assess the rice blast disease severity. In 2021, Kirtphaiboon et al. [5] simulated several locations in Thailand under varied weather

conditions, including temperature and rain. The results showed that the main factor affecting the disease severity was the temperature. Besides, low temperatures and high humidity also caused high disease severity. On the other hand, disease severity is low when temperatures are high and humidity is low. Additionally, the model can forecast the regional distribution of disease severity and the timing of outbreaks under specific climatic conditions. Kapoor et al. [6] investigated the prediction of rice blast disease in Himachal Pradesh's Kangra district in 2004. They discovered that the overall severity of the rice blast in the Kangra district was mild to moderate from 1997 to 1999. During the rice-growing season, there was a wide range in rainfall quantity and distribution. All three years had temperatures between 18 and 28 degrees Celsius and relative humidity levels greater than 9 hours (>90%), which are the appropriate conditions for disease development. The quantitative prediction equations developed were not useful in forecasting rice blast disease because no variables such as temperature, wetness duration, rainy days, and hours of relative humidity (>90%) were supported. However, spore dispersal has not been studied in either literature.

A diffusive mathematical model can describe the spread of an infectious disease within a human, plant, and computer [7]. Modeling the evolution dynamics of infectious diseases requires Partial Differential Equations (PDE), known as reaction-diffusion systems [8]. In the same way, spore dispersion also requires PDE to describe the behavior dispersal. The spore dispersal was studied by Jarroudi et al. [3] in 2020. They proposed a mathematical model to simulate spore dispersal by the wind and the density of a healthy host. The non-local diffusion equation incorporates the non-local factor and the dispersal kernel, simulated spore dispersal, and the wind component contained in the dispersal kernel. According to the findings, spore dispersal by wind induces spore liberation, dependent on wind velocity. The wind direction angle, spore weight, and spore shape are all factors that influence the aerial distribution of spores throughout plant fields. In 2022, Tabonglek et al. [9] proposed a mathematical model for spore dispersal, adding the weather factors to Jarroudi's model but not separating the host populations to other stages. However, the disease severity has not been considered in both papers. In 2008, Buries et al. [10] examined the spatiotemporal spread of a fungal disease over a vineyard using an Susceptible-Exposed-Infected-Removed (SEIR) model coupled with a set of describing spore dispersal. The model accounts for short and long-range spore dispersal and foliar surface growth. This work did not include the weather factors.

Following the above discussions, no studies have been reported on rice blast disease's severity and the distribution of spores influenced by climatic factors at the same time. The host population should be separated into healthy, latent, infectious, and removed to correspond as possible with reality. Therefore, this work aims to extend a mathematical model to assess the severity of rice blast outbreaks that are currently occurring by separating the host population into the healthy host, latent, infectious, and removed with the PDE that describes the spore dispersion from Tabonglek et al., 2022.

2. Methodology

This paper extends the spore dispersal model in Tabonglek et al. [9] to the HLIR epidemic model based on the SEIR model. After that, we used the FDM to estimate the solution. Subsequently, we simulated the disease severity for rice blast disease using meteorological data from the PRRC. Finally, we evaluated the severity of rice blast disease using Willmott's index of agreement [11, 12].

2.1. Disease severity of rice blast

The disease severity (y) is a percentage of symptoms or lesions which causes by the disease, and it considers the area or proportion of symptomatic plant tissue. The diseased leaf area measures the disease severity over the whole leaf area since this research is interested in the HLIR model with the spore dispersal equation. Therefore, the whole area is equal to the sum of the densities of the healthy host, latent, infectious, and removed. In addition, the disease leaf area is equal to the combined densities of the latent and infectious. Finally, the percent disease severity at time t and position x can be calculated from:

$$y(x,t) = \frac{L(x,t) + I(x,t)}{H(x,t) + L(x,t) + I(x,t) + R(x,t)} \times 100, \tag{2.1}$$

where $y(x,t)$ is the disease severity at time t and position x. $H(x,t)$, $L(x,t)$, $I(x,t)$, and $R(x,t)$ are the densities of healthy host, latent, infectious, and removed at time t and position x, respectively. Before assessing the disease severity of rice blast disease, we must find the densities of a healthy host, latent, infectious, removed at time t and position x from the model in the following section.

2.2. Model extension

The mathematical model for spore dispersion via wind and rain is described by Tabonglek et al. [9]. Assume that time t and position x are both continuous variables which x belong to a bounded domain $\Omega \subset \mathbb{R}$ and $t > 0$. The rate of change in the densities of healthy host and spore are described by Eqs (2.2) and (2.3), respectively.

$$\frac{\partial H(x,t)}{\partial t} = -\alpha(t)u(x,t)H(x,t), \tag{2.2}$$

$$\frac{\partial u(x,t)}{\partial t} = \int_{\Omega} J(x-y)[u(y,t) - u(x,t)]dy + f(x,t), \tag{2.3}$$

$$H(x,0) = H_0(x) \geq 0, \tag{2.4}$$

$$u(x,0) = u_0(x) \geq 0. \tag{2.5}$$

The Eq (2.2) is only a healthy host's reduction due to infection, and Eq (2.3) depends on spore dispersal and spore production. Where $H(x,t)$ and $u(x,t)$ are densities of healthy host and spore at time t and position x, respectively. $\alpha(t)$ is the proportion of the plant that will become infected at time t. $J(x-y)$ is the probability of a pathogen migrating from location y to the position x, and $f(x,t)$ is the spores production by infectious hosts or lesions at time t and position x. The proportion of infecting a susceptible individual at time t ($\alpha(t)$) can be calculated from the Eq (2.6):

$$\alpha(t) = \mu \cdot \varphi_{max} \cdot \varphi_T(t) \cdot \varphi_D(t), \tag{2.6}$$

where μ is the fraction of spore deposition on the crop, φ_{max} is the maximum infection efficiency, $\varphi_T(t)$ and $\varphi_D(t)$ are the infection efficiency based on the temperature and dew period at a time t, respectively. The infection efficiency is the proportion of spores that can infect and cause lesions after spores fall on susceptible host tissue. Which the infection efficiency depending on temperature at time t ($\varphi_T(t)$) [5] can be describe in Eq (2.7):

$$\varphi_T(t) = \left(\frac{T(t) - T_{IEmin}}{T_{IEmax} - T_{IEmin}}\right)^{x_{IE}} \left(\frac{T_{IEmax} - T(t)}{T_{IEmax} - T_{IEmin}}\right)^{y_{IE}}, \tag{2.7}$$

where $T(t)$ is the daily temperature, T_{IEmax} is the maximum temperature, T_{IEmin} is the minimum temperature, and x_{IE}, y_{IE} are constants. The infection efficiency depending on dew period at time t ($\varphi_D(t)$) [5] can be describe in Eq (2.8):

$$\varphi_D(t) = 1 - e^{-d_1(D(t)-W_{min})}, \tag{2.8}$$

where $D(t)$ is the daily relative humidity, W_{min} is the minimum wetness period of the infection efficiency, and d_1 is constant.

The probability that a spore migrates from position y to position x by wind and rain can be described in Eq (2.9). This term corresponds to the density probability function. In 1999, van den Bosch et al. [13] explained that the spore dispersal distribution is approximated by exponential distribution and Bessel density. Since Bessel's graph is higher than the exponential graph (see Figure 2 in [13]), the spores tend to concentrate, making them less diffuse than the exponential density. In addition, the average flight time $(1/\mu)$ is relatively tiny compared to the average airflow duration $(1/\gamma)$ in a fixed direction. The spores fall far from their source. Therefore, the spore dispersal is approximated by the exponential distribution [3, 13]. On the other hand, the Bessel function estimated the spore dispersion when the amount of time a spore spends in the wind $(1/\mu)$ exceeds the time it spends migrating in a fixed direction $(1/\gamma)$. The wind blows the spores back down near the source.

$$J(x-y) = \begin{cases} \dfrac{\mu^2}{2\pi(Fv_1+v_2)^2}\exp\left(-\dfrac{\mu}{Fv_1+v_2}|x-y|\right) & \text{if } \mu > \gamma, \\ \dfrac{\mu^2}{8\pi(Fv_1+v_2)^2}K_0\left(\dfrac{\mu}{(Fv_1+v_2)\sqrt{2}}|x-y|\right) & \text{if } \mu < \gamma, \end{cases} \tag{2.9}$$

where $J(x-y)$ is the probability of a pathogen migrating from location y to the position x. v_1 is the velocity of fluid fragmentation after rainfall on the host, v_2 is the wind velocity, and F is the probability of rain in the day. If there is rain, $F = 1$ denotes that wind and rain play a role in spore spreading. Furthermore, if there is no rain, $F = 0$, the spore dispersal depends on wind only.

The spores production by lesions at time t, position x ($f(x,t)$) is the number of spores produced by lesions or infectious hosts per unit of time at position x, which can be computed as follows:

$$f(x,t) = \kappa \int_0^t u(x,t-s)H(x,t-s)\alpha(s)\beta(s)ds, \tag{2.10}$$

where κ is the average number of spores produced per lesion until the start removal stage, $\alpha(s)$ is the proportion of infecting a healthy host at time s, and $\beta(s)$ is the sporulation curve at time s, which can be expressed as Eq (2.11):

$$\beta(s) = \begin{cases} 0 & \text{if } s < \tau, \\ \dfrac{a^b(s-\tau)^{b-1}e^{-a(s-\tau)}}{\Gamma(b)} & \text{if } s \geq \tau, \end{cases} \tag{2.11}$$

where τ is the latent period, s is the age of infection, Γ is the gamma function, and a, b are constants. The age of infection begins when the spore penetrates the host tissue through sporulation and enters the latent stage.

Model in Eqs (2.2) and (2.3) considered the densities of healthy host and spore, focusing on the spore dispersal. The spores are active, inactive, or have penetrated plant tissues but do not show

lesions. We count them all as the spores density. To correspond to the real situation, we will separate the host populations into the HLIR model. Since plant populations can senescence at each stage, the extended model will include a term about senescence. The flow diagram for the disease dynamics with compartments H, L, I, R, and u is given in Figure 1.

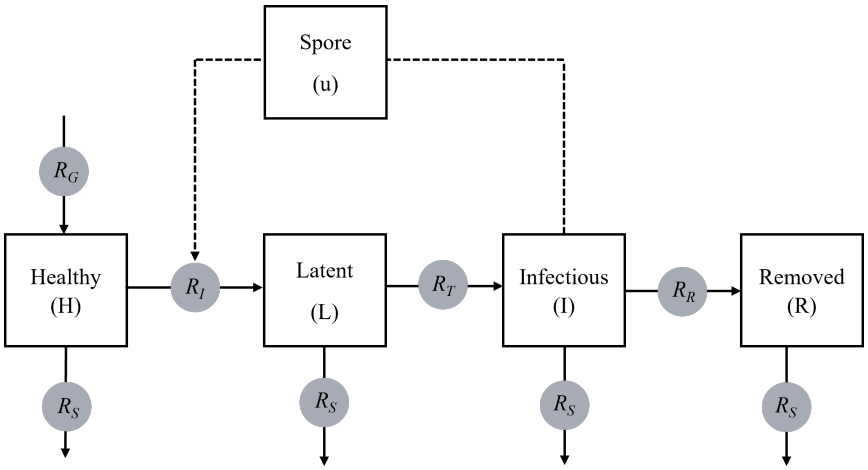

Figure 1. Diagram of the extended model.

Figure 1 illustrates the flow diagram for the disease dynamics, in which the arrows represent the host population changes. If the arrow points out from the compartment meaning that the population or the density decreases, whereas the arrow points to the compartment, meaning that the density increases. R_G, R_I, R_T, R_R, and R_S are the rates of growth, infection, transmission, removal, and senescence, respectively. Let the total density $N(x,t) = H(x,t) + L(x,t) + I(x,t) + R(x,t)$. The rate of senescence will appear in all stages of host populations. Moreover, leaf senescence will appear in the last stage of plant development and is influenced by various genetic and environmental variables. Because of the loss of green pigment chlorophyll, leaf yellowing is a visible sign of senescence [14]. Therefore, the rate of senescence term contained the Heaviside function, which can be calculated from:

$$h(t - t_s) = \begin{cases} 1, & t > t_s, \\ 0, & t \leq t_s, \end{cases} \tag{2.12}$$

this function controls the senescence term, which appears when daily time is more than the time of senescence ($t > t_s$).

The epidemic of rice blast disease had no impact on population growth. Moreover, the general model separates into two parts: population growth and disease epidemic. Population growth involves the growth rate and the senescence rate. Therefore, the change in total population can be described as follow:

$$\frac{\partial N(x,t)}{\partial t} = r_G N(x,t)\left(1 - \frac{N(x,t)}{K_G}\right) - 2h(t - t_s)r_s(H(x,t) + L(x,t) + I(x,t)), \tag{2.13}$$

where $N(x,t)$, $H(x,t)$, $L(x,t)$, and $I(x,t)$ are the densities of total, healthy, latent, and infectious at time t and position x, respectively. r_G is the relative rate of growth, K_G is the carrying capacity, r_s is the relative rate of senescence, $h(t - t_s)$ is the Heaviside function, and t_s is date of senescence.

Firstly, the rate of change of healthy host individuals is considered with respect to time t. Healthy host density changes depending on three terms: growth, infection, and senescence. For the growth rate, we used logistic growth because rice has limited growth. The infection rate was calculated using the same component in Tabonglek et al. because this term is based on the weather variable. Therefore, we can write the PDE as follows:

$$\frac{\partial H(x,t)}{\partial t} = \underbrace{r_G N(x,t)\left(1 - \frac{N(x,t)}{K_G}\right)}_{R_G} - \underbrace{\alpha(t)u(x,t)H(x,t)}_{R_I} - \underbrace{h(t-t_s)r_s H(x,t)}_{R_S}, \tag{2.14}$$

where $H(x,t)$, $u(x,t)$, and $N(x,t)$ are the densities of healthy host, spore, and total, respectively at time t and position x. r_G is the relative rate of growth, K_G is the carrying capacity, r_s is the relative rate of senescence, t_s is date of senescence, and $\alpha(t)$ is the proportion of plant that will become infected at time t. The second considers the latent density change rate with respect to time t depending on three terms: infection, transmission, and senescence rates. We can write a PDE as Eq (2.15):

$$\frac{\partial L(x,t)}{\partial t} = \underbrace{\alpha(t)u(x,t)H(x,t)}_{R_I} - \underbrace{\frac{1}{\tau}L(x,t)}_{R_T} - \underbrace{h(t-t_s)r_s L(x,t)}_{R_S}, \tag{2.15}$$

where $L(x,t)$ is the latent density at time t and position x and τ is the latent period. The third considers the infectious density change rate with respect to time t depending on three terms: transmission, removal, and senescence. We can write a PDE as Eq (2.16):

$$\frac{\partial I(x,t)}{\partial t} = \underbrace{\frac{1}{\tau}L(x,t)}_{R_T} - \underbrace{\frac{1}{p}I(x,t)}_{R_R} - \underbrace{h(t-t_s)r_s I(x,t)}_{R_S}, \tag{2.16}$$

where $I(x,t)$ is the density of infectious at time t and position x and p is the infectious period. Finally, considering the rate of change of removed density with respect to time t depending on two terms, including the removal rate and the senescence rate from healthy, latent, and infectious because at this stage, we considered removing from disease only given as (2.17):

$$\frac{\partial R(x,t)}{\partial t} = \underbrace{\frac{1}{p}I(x,t)}_{R_R} - \underbrace{h(t-t_s)r_s(H(x,t)+L(x,t)+I(x,t))}_{R_S}, \tag{2.17}$$

where $R(x,t)$ is the density of removed at time t and position x. Since spore dispersal is still important to the epidemic of the disease, we used a structure following Tabonglek et al., 2022 for the spore dispersal with a little-term change. The total density of the spore stands for $u(x,t)$, which is described in the Eq (2.3). Still, we changed the spore production that depends on the healthy host and spore densities to healthy and infectious densities because the spore that can produce a new spore is the spore in the infectious density. Therefore, the spore production can be described by Eq (2.18):

$$f(x,t) = \kappa \int_0^t I(x,t-s)H(x,t-s)\alpha(s)\beta(s)ds. \tag{2.18}$$

Hence, the rate of change of spore density with respect to time t can describe in Eq (2.19):

$$\frac{\partial u(x,t)}{\partial t} = \int_{\Omega} J(x-y)[u(y,t)-u(x,t)]dy + f(x,t). \tag{2.19}$$

The model for the epidemic of rice blast disease is described by the system of Eqs (2.20)–(2.24):

$$\begin{aligned}
\frac{\partial H(x,t)}{\partial t} &= r_G N(x,t)\Big(1-\frac{N(x,t)}{K_G}\Big) - \alpha(t)u(x,t)H(x,t) - h(t-t_s)r_s H(x,t), && (2.20)\\
\frac{\partial L(x,t)}{\partial t} &= \alpha(t)u(x,t)H(x,t) - \frac{1}{\tau}L(x,t) - h(t-t_s)r_s L(x,t), && (2.21)\\
\frac{\partial I(x,t)}{\partial t} &= \frac{1}{\tau}L(x,t) - \frac{1}{p}I(x,t) - h(t-t_s)r_s I(x,t), && (2.22)\\
\frac{\partial R(x,t)}{\partial t} &= \frac{1}{p}I(x,t) - h(t-t_s)r_s\big(H(x,t)+L(x,t)+I(x,t)\big), && (2.23)\\
\frac{\partial u(x,t)}{\partial t} &= \int_{\Omega} J(x-y)[u(y,t)-u(x,t)]dy + f(x,t). && (2.24)
\end{aligned}$$

For $x \in \Omega$ and $t > 0$ with nonnegative initial conditions: $H(x,0) = H_0(x) \geq 0, L(x,0) = L_0(x) \geq 0, I(x,0) = I_0(x) \geq 0, R(x,0) = R_0(x) \geq 0$, and $u(x,0) = u_0(x) \geq 0$.

2.3. Numerical solutions

In this work, we want to forecast future disease severity using past data. Therefore, we selected a forward finite difference or explicit method to solve the model. First, set the domains $\Omega = [0,1]$ and $t = [0,100]$, and then discretize time into $N_t = 100$ intervals and discretize space into $N_x = 100$ intervals as illustrated in Figure 2. The space step size denoted by δx and the time step size denoted by δt are equal to 0.01 and 1, respectively. Assume that H_i^j, L_i^j, I_i^j, R_i^j and u_i^j are approximations of $H(x_i,t_j)$, $L(x_i,t_j)$, $I(x_i,t_j)$, $R(x_i,t_j)$, and $u(x_i,t_j)$, respectively.

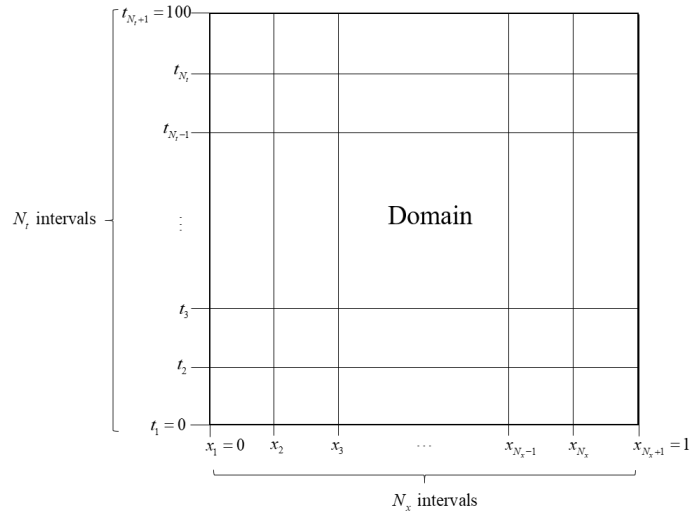

Figure 2. Discretization of time t and spatial x.

We can write the Eqs (2.20)–(2.24) to the vector Eq (2.25):

$$\frac{\partial \mathbf{U}}{\partial t} = \mathbf{F}(\mathbf{U}), \tag{2.25}$$

where

$$\mathbf{U} = \begin{bmatrix} H \\ L \\ I \\ R \\ u \end{bmatrix} \text{ and } \mathbf{F}(\mathbf{U}) = \begin{bmatrix} r_G N\left(1 - \frac{N}{K_G}\right) - \alpha u H - h r_s H \\ \alpha u H - \frac{1}{\tau} L - h r_s L \\ \frac{1}{\tau} L - \frac{1}{p} I - h r_s I \\ \frac{1}{p} I - h r_s (H + L + I) \\ \int_\Omega J(x-y)[u(y,t) - u(x,t)]dy + f \end{bmatrix}.$$

The Eq (2.24) includes the integral terms. The first term and second terms can approximate to Eqs (2.26) and (2.27), respectively.

$$\left(\int_\Omega J(x-y)[u(y,t) - u(x,t)]dy \right)_i^j \approx \sum_{p=1}^{N_x+1} J(x_i - x_p)(u_p^j - u_i^j)\delta x, \tag{2.26}$$

where $i = 1, 2, 3, ..., N_x + 1$ and $j = 1, 2, 3, ..., N_t + 1$. The second term of the right-hand-side is called the spore production and is approximated as follows:

$$f_i^j = \left(\kappa \int_0^t I(x, t-s) H(x, t-s) \alpha(s) \beta(s) ds \right)_i^j \approx \kappa \sum_{l=1}^{j} \alpha^l \beta(t_j - t_l)(IH)_i^j \delta t, \tag{2.27}$$

where $i = 1, 2, 3, ..., N_x + 1$ and $j = 1, 2, 3, ..., N_t + 1$. After that, substitute Eqs (2.26) and (2.27) into the integral terms and approximate the Eq (2.25) using explicit method, we get:

$$\begin{aligned} \frac{\mathbf{U}_i^{n+1} - \mathbf{U}_i^n}{\delta t} &= \mathbf{F}_i^n \\ \mathbf{U}_i^{n+1} &= \mathbf{U}_i^n + \delta t \mathbf{F}_i^n \end{aligned} \tag{2.28}$$

or

$$\begin{bmatrix} H \\ L \\ I \\ R \\ u \end{bmatrix}_i^{n+1} = \begin{bmatrix} H \\ L \\ I \\ R \\ u \end{bmatrix}_i^{n} + \delta t \begin{bmatrix} r_G N_i^n \left(1 - \frac{N_i^n}{K_G}\right) - \alpha^n u_i^n H_i^n - h r_s H_i^n \\ \alpha^n u_i^n H_i^n - \frac{1}{\tau} L_i^n - h r_s L_i^n \\ \frac{1}{\tau} L_i^n - \frac{1}{p} I_i^n - h r_s I_i^n \\ \frac{1}{p} I_i^n - h r_s (H + L + I)_i^n \\ \sum_{p=1}^{N_x+1} J(x_i - x_p)(u_p^j - u_i^j)\delta x + \kappa \sum_{l=1}^{j} \alpha^l \beta(t_j - t_l)(IH)_i^j \delta t \end{bmatrix},$$

for every $i = 1, 2, 3, ..., N_x + 1$ and $n = 1, 2, 3, ..., N_t$.

2.4. Data

This section will present the data used in this research, which can be divided into three primary categories: environmental data, disease severity data, and parameter data.

2.4.1. Environmental data

Temperature (T), relative humidity (D), and rain (R) were the three types of environmental data used in this research. We got all data from the PRRC, which considered two beds. The average temperature in bed 1 was 27.23 $^{\circ}C$, while the range was 24.2–34.65 $^{\circ}C$. The relative humidity ranged from 68 to 91.5%, with the mean value being 81.84%. The average rainfall was 6.53 mm, the highest rainfall was 71 mm, and the lowest rainfall was 0 mm. The data are shown in Figure 3(a). For bed 2, the mean temperature was 26.02 $^{\circ}C$, and the temperature was between 17.7–29.2 $^{\circ}C$. The mean relative humidity was 71.52%, and the relative humidity was between 47–84.5%. Mean rain was 0.08 mm, the maximum rain was 5.8 mm, and the minimum rain was 0 mm. The data are shown in Figure 3(b).

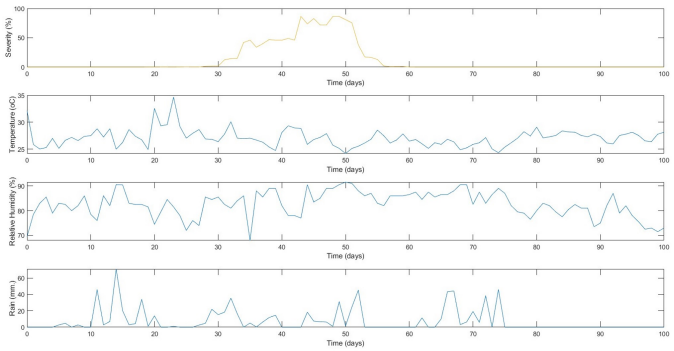

(a)

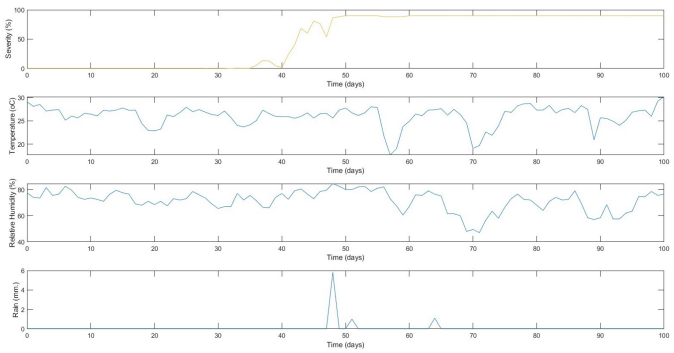

(b)

Figure 3. Environmental data for the period between 28 July 2015 and 25 November 2015 from PRRC. (a) Bed 1 and (b) bed 2.

2.4.2. Disease severity data

We obtained disease severity data from the PRRC. Bed 1, the rice blast outbreak date is 16 August 2015–2 October 2015 (day 20–day 67). The disease severity on day 20 is 0.12%, day 67 is 0.02%, and the maximum disease severity is 86.4%, shown in the top box of Figure 3(a). Bed 2, the

rice blast outbreak date is 23 December 2015–7 March 2016 (day 25–day 100). The disease severity on day 25 is 0.04%, day 100 is 90%, and the maximum disease severity is 90%, shown in the top box of Figure 3(b).

2.4.3. Parameters data and initial conditions

The initial conditions: $H_0(x) = 0.015$ (fitted from LAI), $L_0(x) = I_0(x) = R_0(x) = 0$, and $u_0(x) = 0$ are used for simulation and all parameters shown in Table 1.

Table 1. Description and the value of variables and parameters.

Symbol	Description	Value	Source
μ	The fraction of spore deposition on the crop for bed 1	0.173	Modified
	The fraction of spore deposition on the crop for bed 2	0.016	Modified
φ_{max}	The maximum infection efficiency	0.307	[15]
T_{IEmax}	The maximum temperature for bed 1	34.65	PRRC.
	The maximum temperature for bed 2	30.25	PRRC.
T_{IEmin}	The minimum temperature for bed 1	24.2	PRRC.
	The minimum temperature for bed 2	17.7	PRRC.
k_{IE}	The maximum number of infection efficiency	3	[15]
x_{IE}, y_{IE}	Constants	1,0.6	[15]
W_{min}	The minimum wetness period for bed 1	68	PRRC.
	The minimum wetness period for bed 2	47	PRRC.
d_1	Constant	0.1	[15]
v_1	The velocity of fluid fragmentation after rain falls on the host	7	[16]
v_2	The wind velocity	4	[17]
τ	The latent period	5	[18]
κ	The average number of spores produced per lesion	5000	[15]
a, b	Constants	0.24,2.86	[3]
r_G	The relative rate of growth	0.209	[5]
r_s	The relative rate of senescence	0.103	[5]
p	The infectious period	20	[18]
K_G	The carrying capacity	5.524	[5]
t_s	The date of senescence	95	Fitted from LAI

2.5. Model evaluation

Model evaluation is important and helps find the best model with our observation data. We will use Willmott's agreement index to evaluate the model in this work.

Willmott's index of agreement (d), which ranges from 0 to 1, is a standardized indicator of the level of model prediction error. The agreement index demonstrates the potential error ratio and the mean square error. A perfect match is indicated by a value of 1, whereas a value of 0 shows no agreement. Therefore, the index of agreement is expressed as [11, 12]:

$$d = 1 - \frac{\sum_{i=1}^{n}(P_i - O_i)^2}{\sum_{i=1}^{n}(\mid P_i - \bar{O} \mid + \mid O_i - \bar{O} \mid)^2}, \tag{2.29}$$

where d is Willmott's index of agreement. n is the total number of position, P_i is the simulation value at position i, and O_i is the observation value at position i.

3. Results

3.1. Densities of healthy host, latent, infectious, removed, and spore

We used the numerical solution from Eq (2.28) and all the values for the variables and parameters in Table 1 to simulate the epidemic model for rice blast disease. Moreover, we calculated it using MATLAB software version R2022a (license 40844420), and the curves were simulated for 100 days. The results of simulations are shown in Figures 4 and 5 for beds 1 and 2, respectively. Tabonglek et al. [9] considered two densities: a healthy host and a spore. While this research, we separated the host populations into healthy, latent, infectious, and removed with spore density. The initial condition of a healthy host is $H_0(x) = 0.015$ while the latent, infectious, removed, and spore are equal to zero ($L_0(x) = I_0(x) = R_0(x) = u_0(x) = 0$) because the disease no occurs. In this research, the disease onset on day 20 after planting means starting a latent period. Therefore, the latent density starts on day 20. After that, we set the latent and spore conditions as $L_{20}(x) = x$ (fitted from observation data) and $u_{20}(x) = 100(1 - x^2)^2$ (from [3]).

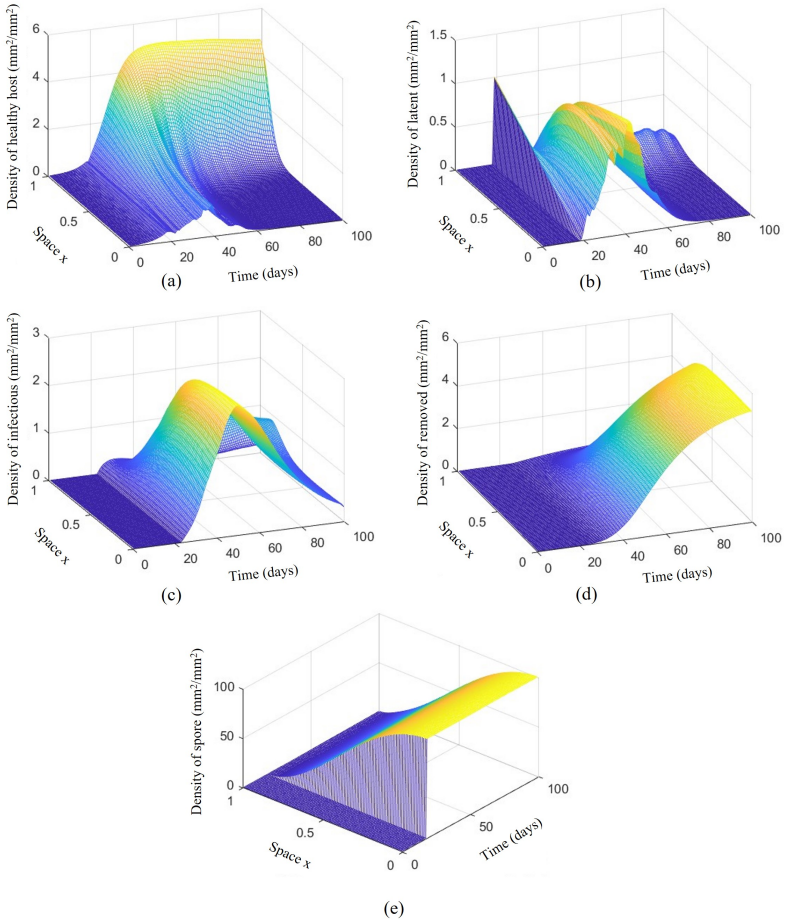

Figure 4. Density curves of epidemic model for rice blast disease in bed 1. (a) Healthy hosts individual, (b) latent, (c) infectious, (d) removed, and (e) spore.

Figures 4 and 5 illustrate the result from simulation in beds 1 and 2, respectively that including

the densities of a healthy host, latent, infectious, removed, and spore are shown in sub-figures (a)–(e), respectively. The x-axis stands for time t, which ranges from 0 to 100 days, the y-axis stands for space x, considered one unit, and the z-axis stands for the densities of all stages. In all beds, The host population density will not exceed the carrying capacity (K_G). The healthy host density increases by the growth stages to the peak value and decreases to zero. After the disease onset, the latent and infectious density curves are in the same direction, and the removed density increases to the peak value until the end crop. In addition, the spore density curve rises to a high level till the end of the process.

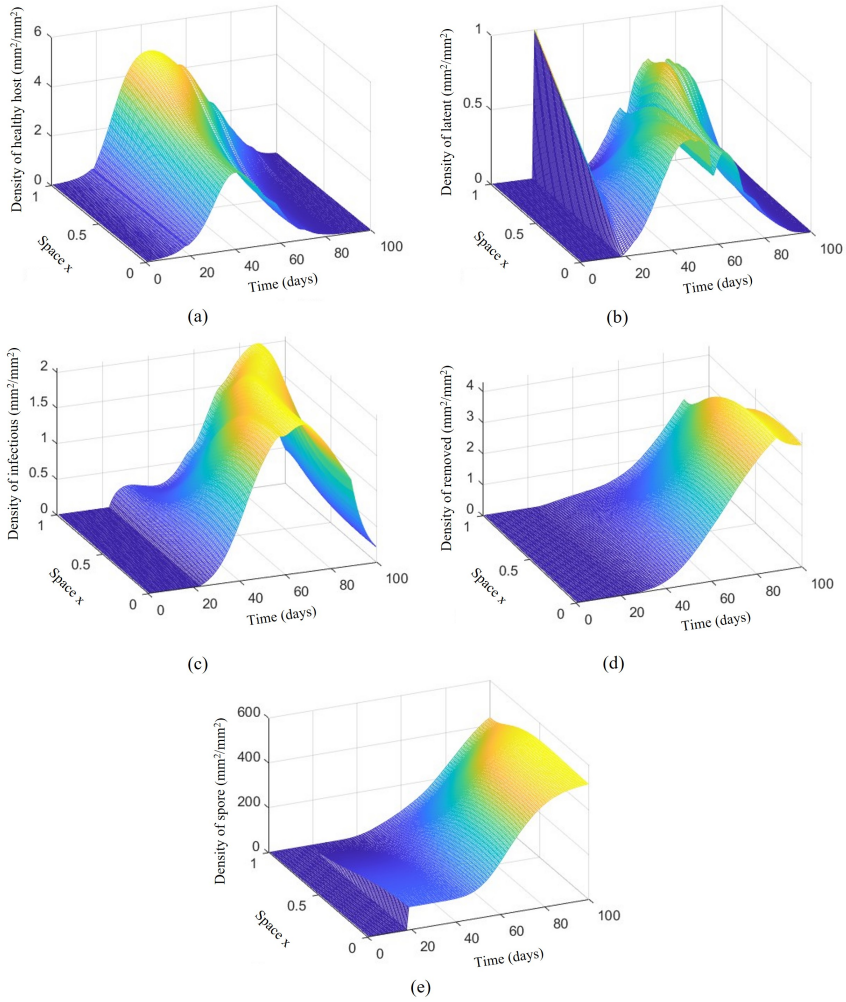

Figure 5. Density curves of epidemic model for rice blast disease in bed 2. (a) Healthy hosts individual, (b) Latent, (c) infectious, (d) removed, and (e) spore.

3.2. Percent disease severity

In section 2.3, we got the densities of the healthy host, latent, infectious, and removed. After that, we simulated the rice blast disease severity, which used the Eq (2.1) with MATLAB software version R2022a (license 40844420) for calculations. The results show in Figure 6. When (a) represents the disease severity for bed 1 and (b) represents bed 2. Both figures show the disease severity of rice blasts. We see that after the disease onset, the disease severity slightly decreases in all beds. After that,

increasing to some value and then decreases to zero.

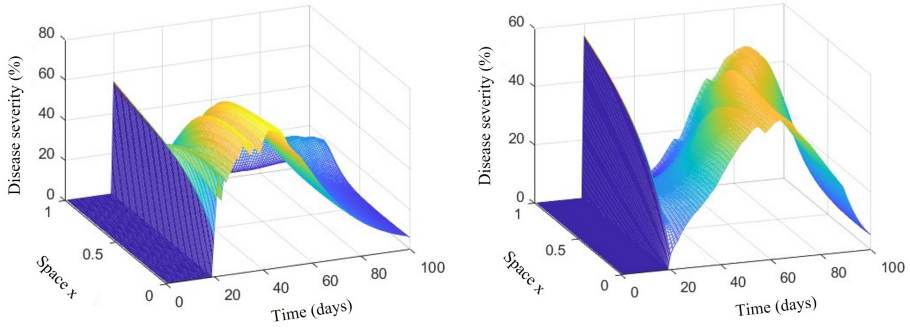

(a) (b)

Figure 6. Density curve of disease severity. (a) Bed 1 and (b) bed 2.

3.3. Adjusted parameter

We modified the parameter's value using their value with the following details. The value of a fraction of spore deposited on the crop was given a number between 0 and 1. Consequently, we varied the value from this interval. For step size of this parameter was considered as 0.001. Then, we substituted each parameter case into the model and calculated the disease severity. After that, we compared the simulated disease severity with the referred disease severity from PRRC. As a result, we received a small error for both beds by looking at Figure 7(a,b).

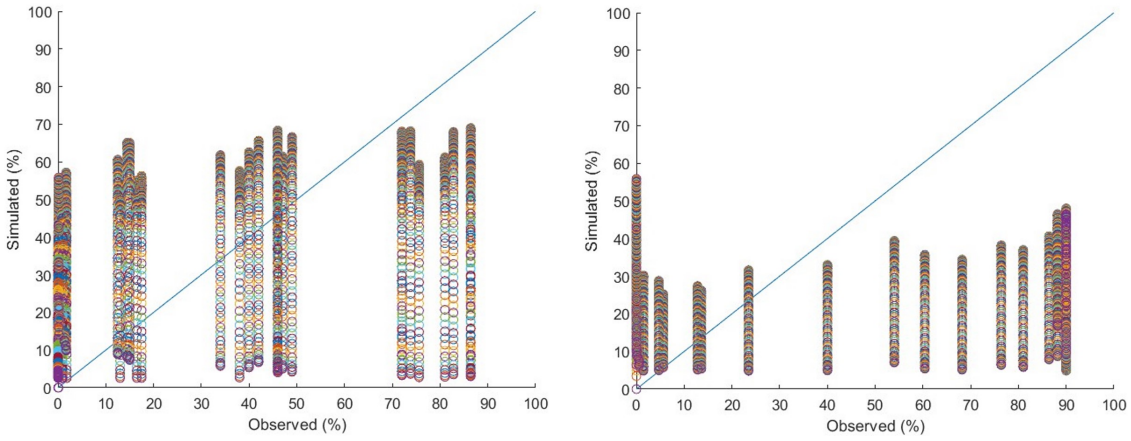

(a) (b)

Figure 7. Scatterplots of simulated and observed datasets of disease severity. (a) Bed 1 and (b) bed 2.

Figure 7 illustrates scatterplots of simulation and observation of disease severity for beds 1 and 2. x-axis represents the observation of disease severity while the y-axis represents the simulation of disease severity. Each dots in the figure are the coordinate of simulated and observed. Suppose each dot is near a 45^o line, which means a small error. Moreover, d values indicate the model performance. In

comparison, bed 1 gave $d = 0.7166$ with a suitable fraction of spore deposited on the crop being 0.173. The result of bed 2, $d = 0.6421$ with a suitable fraction of spore deposited on the crop being 0.016.

4. Discussions

Assessing the severity of rice blast disease can tell the percentage of the infected area. We can devise a plan to deal with the violence if we know the disease severity. Currently, researchers are finding ways to deal with diseases that will spread in rice using a mathematical model to explain. Tabonglek et al., 2022 studied the spore dispersal and the healthy host density affected by climate factors. We expanded Tabonglek's model to make it more realistic by separating the host population into healthy, latent, infectious, and removed stages. Each stage contained the leaf senescence, and the final stage was considered specifically removed from the disease. After that, we simulated the disease severity and compared it with the PRRC data.

The weather and severity data received from the PRRC are daily data. In the research, we study spatial in one dimension, therefore, there are many positions throughout the day, but we do not have severity data on each point. Consequently, we assumed that the data at each point were the same throughout the day. The result shows in Figure 7. For this reason, some simulations and the observation data have high differences affecting the d value. However, when calculating d, $[\sum_{i=1}^{n}(P_i - O_i)^2]/[\sum_{i=1}^{n}(\mid P_i - \bar{O} \mid + \mid O_i - \bar{O} \mid)^2]$ is small, affecting the d value close to 1. Therefore, the result indicates the model's performance.

5. Conclusions

Following the results, the extended model corresponds to the real situation. Moreover, one parameter, a fraction of spore deposited on a crop (μ), was modified to make it more suited for epidemic simulation. The process for modification is mentioned in section 3.3. μ were 0.173 and 0.016 for beds 1 and 2, respectively. These values were received by comparing the disease severity from the model and the disease severity from the PRRC. We chose the suitable μ from a small error by looking at the value of Willmott's index of agreement (d). The d were 0.7166 and 0.6421. Therefore, this parameter improved the referred data, which means a perfect match between simulated and observed. We used the disease severity data from the PRRC, which was collected daily. We assumed the disease severity data at every point was the same, but the value should not be the same. Therefore, our suggestion should be to collect the data at all study area points to improve the model.

Acknowledgments

The authors would like to express the gratitude to the Ministry of Higher Education, Science, Research and Innovation for grant support under the Science Achievement Scholarship of Thailand. In addition, this research project was supported by the Thailand Science Research and Innovation (TSRI). Basic Research Fund: Fiscal year 2022 under project number FRB650048/0164 and Graduate Development Scholarships under the National Research Council of Thailand (NRCT) fiscal year 2021 grant number N41D640010.

Conflict of interest

The authors declare no conflicts of interest.

References

1. D. O. TeBeest, C. Guerber, M. Ditmore, 2007, Rice blast, *The Plant Health Instructor*. https://doi.org/10.1094/PHI-I-2007-0313-07 . Reviewed 2012.
2. N. L. Suriani, D. N. Suprapta, N. Nazir, N. M. S. Parwanayoni, A. A. K. Darmadi, D. A. Dewi, et al., A mixture of piper leaves extracts and rhizobacteria for sustainable plant growth promotion and bio-control of blast pathogen of organic bali rice, *Sustainability*, **12** (2020), 8490. https://doi.org/10.3390/su12208490
3. M. E. Jarroudi, H. Karjoun, L. Kouadio, M. E. Jarroudi, Mathematical modelling of non-local spore dispersion of wind-borne pathogens causing fungal diseases, *Appl. Math. Comput.*, **376** (2020), 1–11.https://doi.org/10.1016/j.amc.2020.125107
4. B. Hau, C. J. de Vallavieille-Pope, Wind-dispersed diseases, In: *The epidemiology of plant diseases*, Netherlands: Springer, 2006.
5. S. Kirtphaiboon, U. Humphries, A. Khan, A. Yusuf, Model of rice blast disease under tropical climate conditions, *Chaos Soliton. Fract.*, **143** (2021), 1–8. https://doi.org/10.1016/j.chaos.2020.110530
6. A. S. Kapoor, R. Prasad, G. Sood, Forecasting of rice blast in Kangra district of Himachal Pradesh, *Indian Phytopathol.*, **57** (2004), 440–445.
7. W. Li, J. Ji, L. Huang, Dynamics of a controlled discontinuous computer worm system, *Proc. Amer. Math. Soc.*, **148** (2020), 4389–4403. https://doi.org/10.1090/proc/15095
8. W. Li, J. Ji, L. Huang, Z. Guo, Global dynamics of a controlled discontinuous diffusive SIR epidemic system, *Appl. Math. Lett.*, **121** (2021), 107420. https://doi.org/10.1016/j.aml.2021.107420
9. S. Tabonglek, U. W. Humphries, A. Khan, Mathematical model for rice blast disease caused by spore dispersion affected from climate factors, *Symmetry*, **14** (2022), 1131. https://doi.org/10.3390/sym14061131
10. J. B. Burie, A. Calonnec, M. Langlais, Modeling of the invasion of a fungal disease over a vineyard, *Model. Simu. Sci. Eng. Tec.*, **2** (2008), 11–21. https://doi.org/10.1007/978-0-8176-4556-4_2
11. C. J. Willmott, S. G. Ackleson, R. E. Davis, J. J. Feddema, K. M. Klink, D. R. Legates, et al., Statistics for the evaluation and comparison of models, *J. Geophys. Res. Oceans*, **90** (1985), 8995–9005. https://doi.org/10.1029/JC090iC05p08995
12. M. H. Ali, I. Abustan, A new novel index for evaluating model performance, *J. Nat. Resour. Dev.*, **4** (2021), 1–9. https://doi.org/10.5027/jnrd.v4i0.01
13. F. van den Bosch, J. A. J. Metz, J. C. Zadoks, Pandemics of focal plant disease, a model, *Phytopathology*, **89** (1999), 495–505. https://doi.org/10.1094/PHYTO.1999.89.6.495

14. S. Lee, C. Masclaux-Daubresse, Current understanding of leaf senescence in rice, *Int. J. Mol. Sci.*, **22** (2021), 1–19. https://doi.org/10.3390/ijms22094515

15. S. Bregaglio, P. Titone, G. Cappelli, L. Tamborini, G. Mongiano, R. Confalonieri, Coupling a generic model to the WARM rice simulator to assess leaf and panicle blast impact in a temperature climate, *Eur. J. Agron.*, **76** (2016), 107–117. https://doi.org/10.1016/j.eja.2016.02.009

16. T. Gilet, L. Bourouiba, Fluid fragmentation shapes rain-induced foliar disease transmission, *J. Roy. Soc. Interface*, **12** (2015), 1–12. https://doi.org/10.1098/rsif.2014.1092

17. O. Singh, J. Bathula, D. K. Singh, Rice blast modeling and forecasting, *Int. J. Chem. Stud.*, **7** (2019), 2788–2799.

18. S. Savary, A. Nelson, L. Willocquet, I. Pangga, J. Aunario, Modeling and mapping potential epidemics of rice disease globally, *Crop Prot.*, **34** (2012), 6–17. https://doi.org/10.1016/j.cropro.2011.11.009

AIMS Press